JOURNAL OF GEOPHYSICAL RESEARCH, VOL. 106, NO. D9, PAGES 10,011–10,021, MAY 16, 2001

Lagrangian reconstruction of ozone column and profile at the Arctic Lidar Observatory for Middle Atmosphere Research (ALOMAR) throughout the winter and spring of 1997-1998

Yvan J. Orsolini and Georg Hansen

Norwegian Institute for Air Research (NILU), Kjeller, Norway

Gloria L. Manney and Nathaniel Livesey

Jet Propulsion Laboratory, California Institute of Technology, USA

Ulf-Peter Hoppe

Norwegian Defence Research Establishment (FFI), Kjeller, Norway

Abstract. We present a Lagrangian model-based technique to reconstruct ozone profile and column in support of the interpretation of ozone lidar observations made at the Arctic Lidar Observatory for Middle Atmosphere Research (ALOMAR). High-resolution ozone profiles as well as column ozone are reconstructed locally at ALOMAR, several times a day, regularly throughout the winter and spring of 1997/1998. The approach consists of calculating a large number of back trajectories to determine the origin of air parcels above ALOMAR and of using satellite observations to determine their ozone content. The blend of satellite observations with limited spatial and temporal coverage, and global gridded meteorological data is akin to a simplified form of data assimilation. The usefulness of the approach is demonstrated by a systematic comparison between reconstructed and observed ozone profiles and column and, in particular, their day-to-day variability. Abrupt changes in reconstructed and observed profile shape are caused by polar vortex displacements, deep intrusions of midlatitude air, or vortex edge filamentation. Prominent laminae are seen in the spring, as the vortex breaks down. Short-lived, large-amplitude total ozone peaks are seen in the model and observations, most prominently in February and March, when they are in excess of 100 Dobson units. They are shown to result from a combination of a lowering of isentropes in the lowermost stratosphere and of advection of ozone-rich air from the base of the polar vortex.

1. Introduction

Ground-based ozone lidars are now routinely used to investigate dynamical and chemical processes affecting the high-latitude lower stratosphere [Bird et al., 1997; Hansen et al., 1997; Neuber, 1997]. The Arctic Lidar Observatory for Middle Atmosphere Research (ALOMAR) on the island of Andoya (69.3°N, 16°E) in northern Norway is often located under the stratospheric polar vortex in winter. The observed ozone profile and column are hence strongly variable owing to polar vortex displacements, and to fine-scale filamention and lamination occurring near the vortex edge [Orsolini et al., 1997; Manney et al., 1998; Hansen and Chipperfield, 1999]. Owing to its location at the extremity of the Atlantic storm track, a strong lower stratospheric ozone variability is also induced by active weather systems and accompanying tropopause level fluctuations [Allen and Reck, 1997; Orsolini et al., 1998a].

In the framework of the Third European Stratospheric Ozone Experiment (THESEO), we have collected a series of ozone profiles at ALOMAR over the winter and spring of 1997/1998. Lidar observations in the Arctic are impaired by adverse weather conditions and cloudiness. Only on 40 days, between November 20, 1997, and May 2, 1998, were observations taken.

The large variability of column ozone in the Arctic is illustrated in Figure 1, which shows column ozone from

Paper number 2000JD900659.
0148-0227/01/2000JD900659$09.00

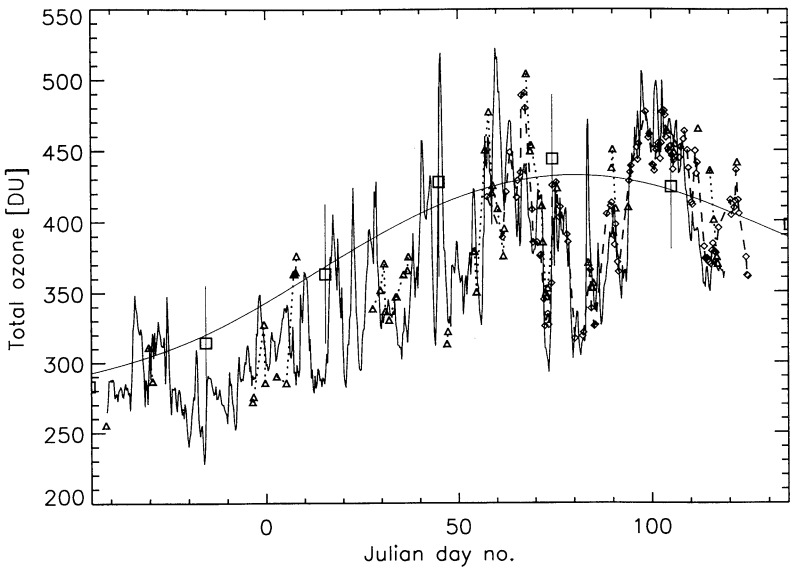

Figure 1. Local total ozone evolution (in Dobson units) throughout the winter and spring of 1997/1998: measurements by the lidar at Andoya (triangles), by the Brewer spectrometer in Tromso (diamonds), and 6-hourly predictions by the model at Andoya (solid line). The smooth seasonal cycle (thin line) fitted to the long-term monthly mean Dobson spectrometer measurements at Tromso (squares) is also shown. Time is labeled in Julian days.

late November 1997 to early May 1998, as determined by the lidar instrument at Andoya (triangles) and by a Brewer spectrometer located at Tromso (69.7°N, 19°E), 130 km away from Andoya (diamonds). While the smooth seasonal cycle (thin line) fitted to the long-term monthly mean Dobson spectrometer measurements at Tromso (squares) shows maximum total ozone in March, there are very large fluctuations on day-to-day or week-to-week time-scales during the winter and spring of 1997/1998, as during any particular winter. Very low column ozone values were observed throughout March 1998, for example. Similarly, the strong variability in ozone lidar profiles is exhibited in Figure 2, which shows lidar profiles as a function of potential temperature on four neighbouring days in early March 1998 (thick black line). The lidar measurements are averaged in 6-hour time bins, centered on standard meteorological times (0000, 0600, or 1800 UT). A large ozone-depleted lamina is seen to appear between March 2 and 3, near 400 K. More details about these measurements and model results will be provided in the rest of the paper, but these observations motivate the modeling approach that we followed.

We have developed an approach based on a back-trajectory model to systematically reconstruct the ozone profile at Andoya throughout the entire winter and spring, in order to examine and understand the variability in ozone profile and column. While there have been numerous observational and modeling studies on lamination in ozone lidar profiles (see the above mentioned references), previous studies have rather focused on case studies.

The method is then used to illustrate various phenomena such as midlatitude intrusions or small-scale laminations. Can the reconstructed profiles display as much variability as observed, in the form of short-lived laminae, for example? We also examine whether the local day-to-day, or week-to-week, variations in column ozone can be reconstructed. The method allows us to discriminate as to whether large and rapid total column ozone increases can solely be attributed to tropopause lowering or whether they also involve horizontal advection of ozone-rich vortex air.

The model uses ozone observations from the 205-GHz radiometer of the Microwave Limb Sounder (MLS) instrument, aboard the Upper Atmosphere Research Satellite (UARS) [e.g., Froidevaux et al., 1994]. This profile reconstruction method uses backward trajectory calculations in the spirit of the trajectory method of Sutton et al. [1994]. It is used here to finely reconstruct an ozone profile and its temporal development, i.e., a vertical time slice at a given location.

The winter of 1997/1998 was on average characterized by higher temperatures and larger wave activity than in preceding years. Despite a strong vortex being established in the first half of December, warming episodes occurred in late December 1997, culminating in a strong warming in early January 1998. After its recovery, the vortex remained small in extent and underwent final breakup after mid-March. The relatively mild winter of 1997/1998 allowed study of pure ozone transport, with insignificant effects due to ozone destruction activated by heterogeneous chemistry. Indeed, little vortex-averaged ClO activation or HNO_3 destruc-

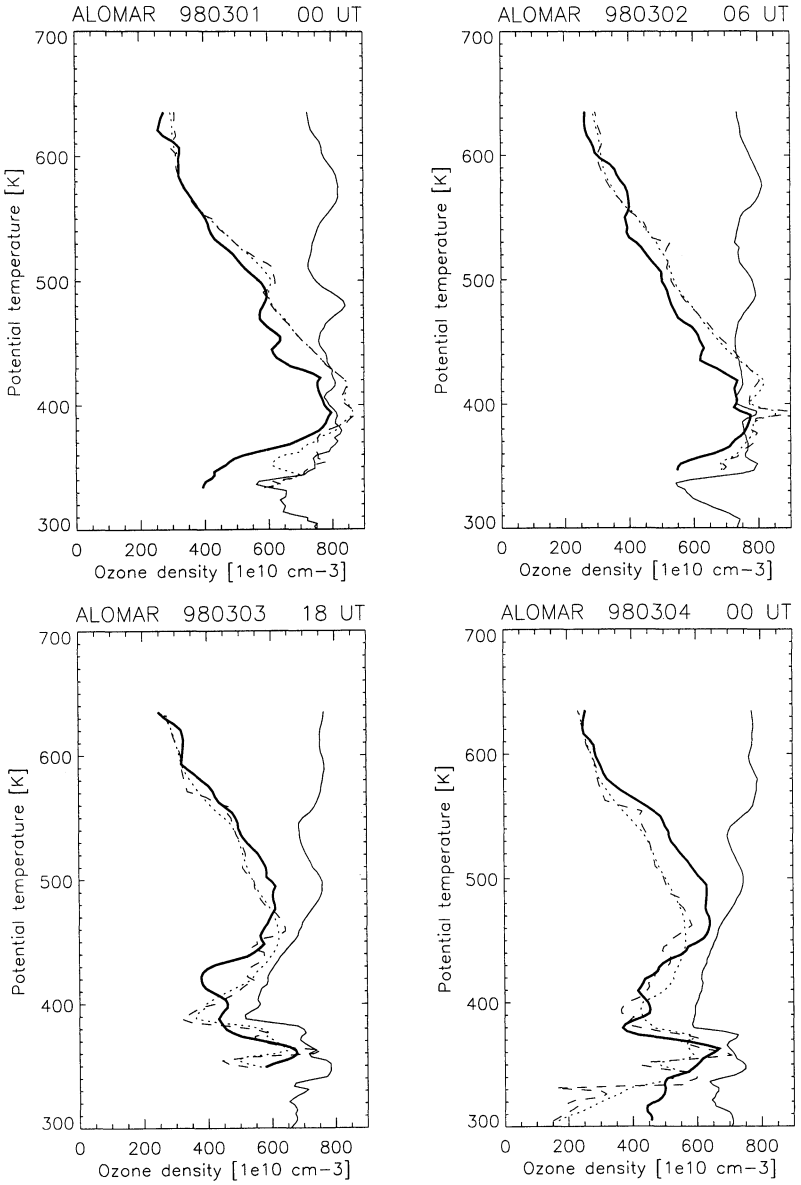

Figure 2. Lidar and reconstructed ozone profiles on March 1-4. In order to better show the low-level variability, the profiles are shown in ozone density rather than in mixing ratio (lidar, thick black line; model at Andoya, dashed line; model box averaged, dotted line). Re-constructed equivalent latitude profiles are also shown (equivalent latitude multiplied by 10, thin black line). Lidar profiles are averaged in 6-hour bins, centered on standard meteorological times (0000, 0600 or 1800 UT).

tion were observed by MLS (M. Santee, personal communication, 1999). Some localized high ClO blobs were nevertheless observed over Scandinavia in late February. There were also few occurrences of polar stratospheric clouds at ALOMAR.

2. Modeling Approach

A reverse domain-filling trajectory model [Manney et al., 1998; Orsolini et al., 1998b] is used to compute isentropic, 8-day backward trajectories starting every 6 hour (0000, 0600, 1200, 1800 UT), in the vicinity of ALOMAR for the period November 21, 1997, to May 1, 1998; 121 trajectories, each representing a parcel of air, are initiated on a regular grid within a 4° by 4° box centered on ALOMAR. These trajectories are calculated on 100 potential temperature (theta) levels between 300 K and 635 K, i.e., from the tropopause to near 25 km. In total, over 8 million back trajectories have been calculated. The winds themselves are interpolated from 31 pressure level European Centre Medium-Range Weather Forecast (ECMWF) analyses, onto 12 theta levels between 300 K and 650 K.

Profiles are hence reconstructed by tagging the par-

cels above Andoya, with ozone at the start of the backward trajectory. The ozone initialization requires the creation of an ozone "catalogue", whereby coarse three-dimensional ozone fields can be looked up every 6 hours. Prototype version 5 MLS data are used here. Froidevaux et al. [1996] described validation of an early version (version 3) of MLS ozone data. The recent version 5 of MLS data gives higher vertical resolution than previous versions and shows smaller biases with respect to correlative data in the lower stratosphere. The MLS data are supplied at equal time intervals along orbit tracks; for use here, these data have been gridded at 4^o latitude by 5^o longitude by binning and taking a weighted average within the bins. Because the MLS data are available only on 31 days, very irregularly spaced, throughout the 5-month period that we investigated, they have been mapped with respect to equivalent latitude [e.g., Manney et al., 1999, and references therein]. This mapping amounts to averaging not along geographical latitudes, but rather along the potential vorticity (PV) contours. The days when MLS made observations are listed in Table 1. A simple linear time interpolation was used across the days when MLS was not observing. MLS data are retrieved on pressure surfaces, the lowest level being 100 mbar. The MLS observations in potential temperature and equivalent latitude coordinates extend down to 375 K. As this isentropic level can fall below 100 mbar, the 375 K ozone is a mixture of observations as well as climatological ozone data described by Froidevaux et al. [1996]. To compute ozone on theta levels below 375 K, a linear interpolation is carried out between the MLS ozone value at 375 K and a value of 50 ppb assigned to the tropopause level, as determined from the analyses.

At this point, one has generated a 6-hourly coarse three-dimensional ozone field. The profiles derived from this field over Andoya are hence smooth; they do not reveal many of the layered structures that are frequently observed by the lidar. Advection, however, generates fine-scale structure from this smooth initial field. The total ozone at Andoya calculated from this MLS-based ozone compares poorly with observed total ozone, owing to the lack of MLS observations below 100 mbar, where ozone structures, e.g., filaments, have a strong impact in the column ozone.

Whenever ozone is to be determined on a particular theta level and at a location on a given day, the equivalent latitude of that location is calculated by using the analyzed potential vorticity. In addition to allowing mapping of the MLS ozone, the equivalent latitude at the start of the trajectories indicates the origin of the air parcel above Andoya.

Table 1. Days of MLS observations during the Winter-Spring of 1997/1998.

MONTH	*DAYS*
November	21, 22, 23, 24, 26, 27, 28, 30
December	1, 2
January	21, 22, 31
February	1, 2, 3, 5, 6, 7, 9, 10, 11, 21, 22
April	16, 17, 18, 19, 30
May	1, 2

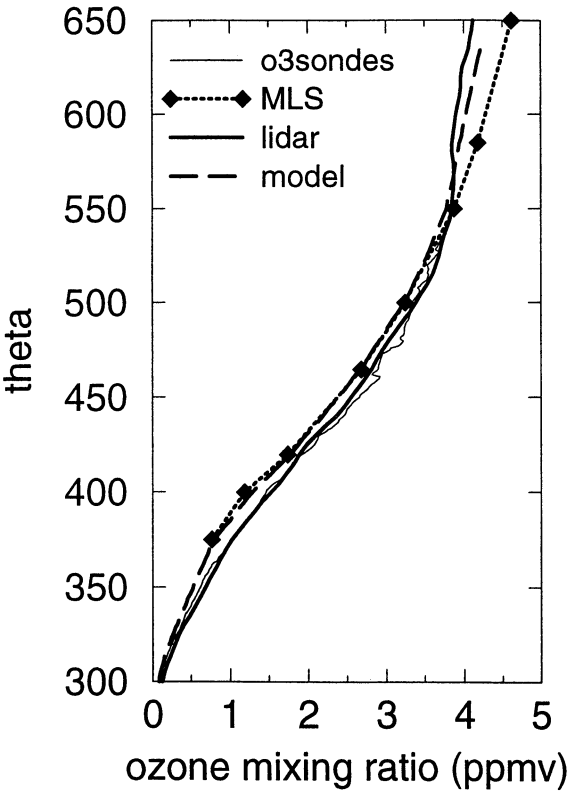

Figure 3. The time means over the winter and spring of 1997/1998 of the lidar, reconstructed MLS, and model ozone profiles at Andoya (in mixing ratio). Also shown is a time mean winter profile determined from ozonesondes launched from Andoya in the winters 1995 to 1999.

3. Measurements of Ozone Profile and Column at Andoya and Tromso

An ozone lidar based on Differential Absorption Lidar (DIAL) technique has been in operation at ALOMAR since 1995. The technical characteristics are described by Hoppe et al. [1995]. Ozone density is derived from the differential absorption of the two wavelengths in an aerosol-free atmosphere, after correction for Rayleigh extinction. The lidar system allows the calculation of an ozone profile from about 10 to 45 km within 1 hour. The altitude sampling is 300 m; a minimum of five values are used to calculate the gradient in the differential absorption profile. Tropospheric ozone is not calculated owing to frequent presence of aerosol and thin cloud layers.

In order to derive total ozone values, the column from the ground to the lowest lidar altitude accepted (typically 10 km) is taken from the closest ozonesonde measurement available, usually from Sodankyla (Fin-

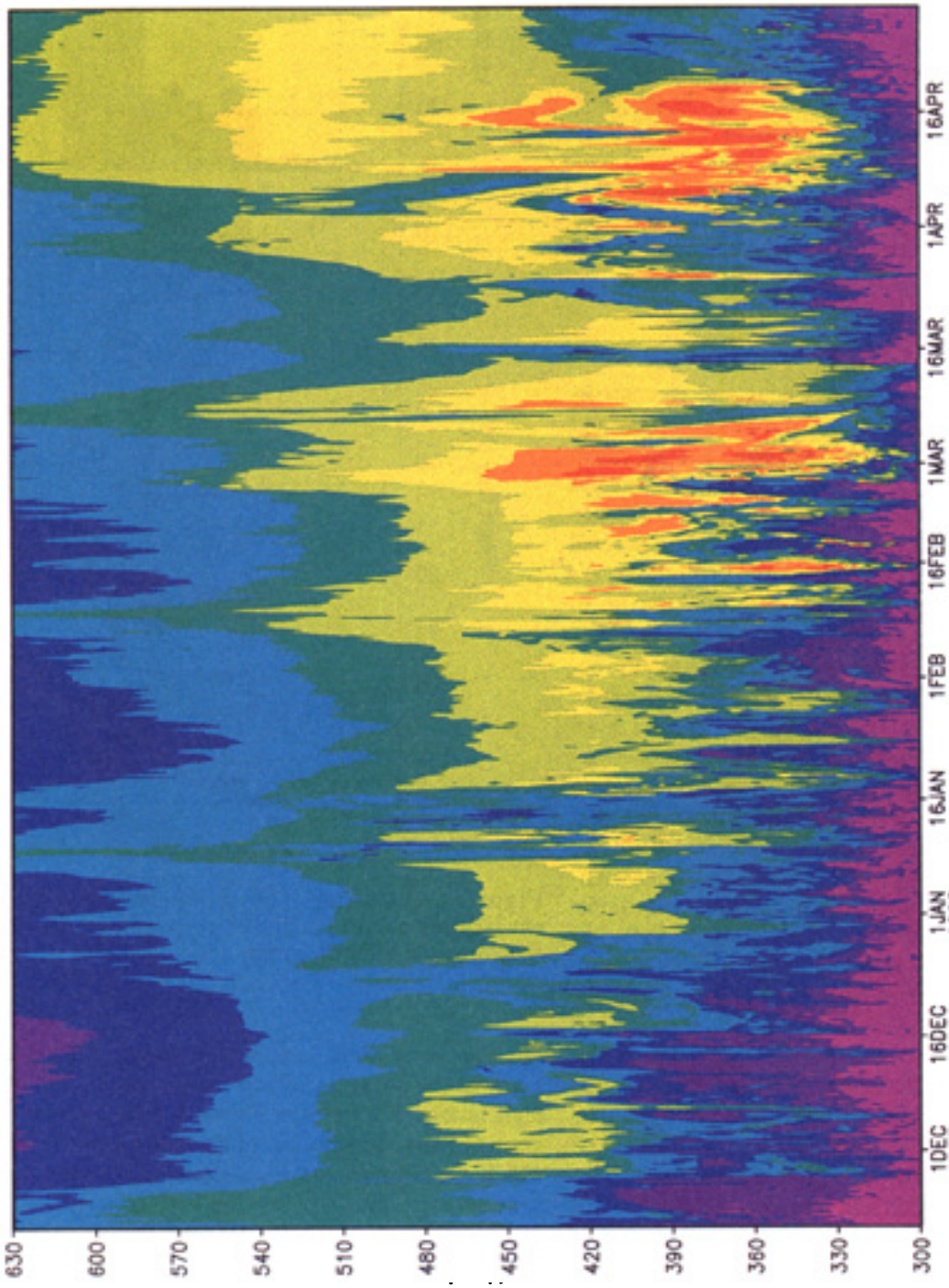

Plate 1. Time evolution of the model ozone profiles at Andoya in partial pressure (mPa) versus potential temperature, throughout the 1997/1998 winter and spring.

land) and, in some cases, from Andoya. Lidar data are used up to typically 35 km; above that altitude, a constant mixing ratio derived from the 30 to 35-km range is assumed. Though this is a very crude assumption (i.e., the mixing ratio reaches a maximum around 35 km and decreases rapidly above 40 km), it is sufficient. The assumed average mixing ratio is smaller than the maximum value, so that the overestimation above, say, 40 km compensates for the underestimation at the mixing ratio maximum. The column from 35 to 50 km is then calculated by using the air density derived from the lidar backscatter profile.

In Tromso, total ozone has been measured on a regular basis for more than 60 years. In this study, we used measurements made with a Brewer spectroradiometer used for routine ozone monitoring.

4. Reconstructed Ozone Profiles

Figure 3 shows the time-mean lidar and reconstructed model profiles (in mixing ratio) over the winter and spring of 1997/1998. For comparison, a time mean winter profile determined from a set of 25 ozonesondes launched from Andoya in the winters 1995 to 1999 and a time mean profile near Andoya from the MLS-derived "ozone catalogue", i.e., before backward transport, are shown as well. The modeled profiles and the MLS-derived profiles slightly underestimate the lidar profiles, throughout the 300 K-650 K layer, but especially below 400 K. On the other hand, there is good agreement between the lidar and ozonesonde profiles even below 400 K. Referring back to Figure 2, the reconstructed ozone and equivalent latitude profiles are shown on March 1 (OOOO UT), 2 (0600 UT), 3 (1800 UT), and 4 (OOOO UT), along with the lidar profiles. Both the highly laminated reconstructed ozone profiles above Andoya (dashed line) and the smoother box-averaged profile around Andoya (dotted line) are shown on each day. The equivalent latitude profile (thin line) has been multiplied by 10 to fit on the figure. The abrupt appearance of a prominent ozone-depleted lamina near 400 K on March 3 is reproduced by the model, which further indicates that midlatitude air (equivalent latitude near 50) was advected above Andoya in that layer. The overall shapes of the profiles, which change from day to day, are reproduced, although many small model laminae have different heights and magnitudes than the observed ones. Laminae statistics will be examined in section 6.

The high variability in model ozone profile at Andoya is vividly illustrated by Plate 1, which shows the time evolution of the model ozone profiles (in partial pressure) throughout the 1997/1998 winter and spring. As Andoya is often under the polar vortex, there is a slow ozone buildup with time as inner vortex ozone increases throughout winter owing to downward transport. In the first part of the winter, the height of the ozone maximum is near 440 K, but higher ozone values

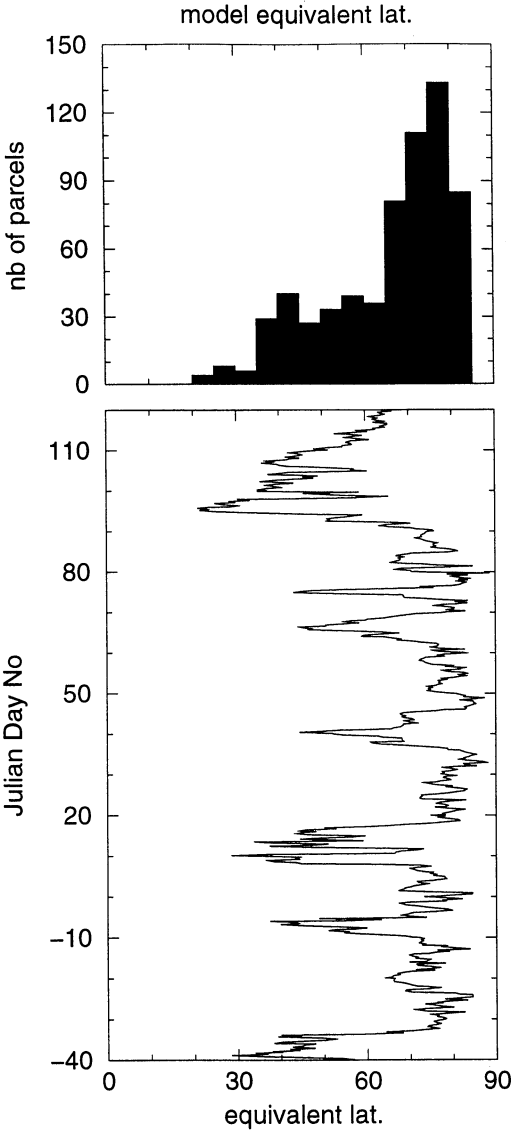

Figure 4. Histogram of the distribution of the equivalent latitude at 475 K. The corresponding time-series is shown below the histogram.

are seen lower down later in the season. The fact that many of the 8-day backward trajectories originate from high latitudes is seen in Figure 4, which shows histograms of the distribution of the equivalent latitude at 475 K throughout the simulation. The corresponding time series is shown below the histogram. Parcels originate most often from equivalent latitudes poleward of 65° N; they also originate from any latitude in the midlatitude surf zone. Rarely before late spring do parcels originate from the subtropics (at 475 K). The intrusions from midlatitudes are very sharply defined.

During lower-latitude intrusions, rapid changes in the profile can occur in fact over the whole modeled layer. Such intrusions bring high-ozone air above about 550 K, and low-ozone air under 550 K. Several such high-ozone pulses are clearly seen in January or February, for example, at 550 K near January 10 or February 12

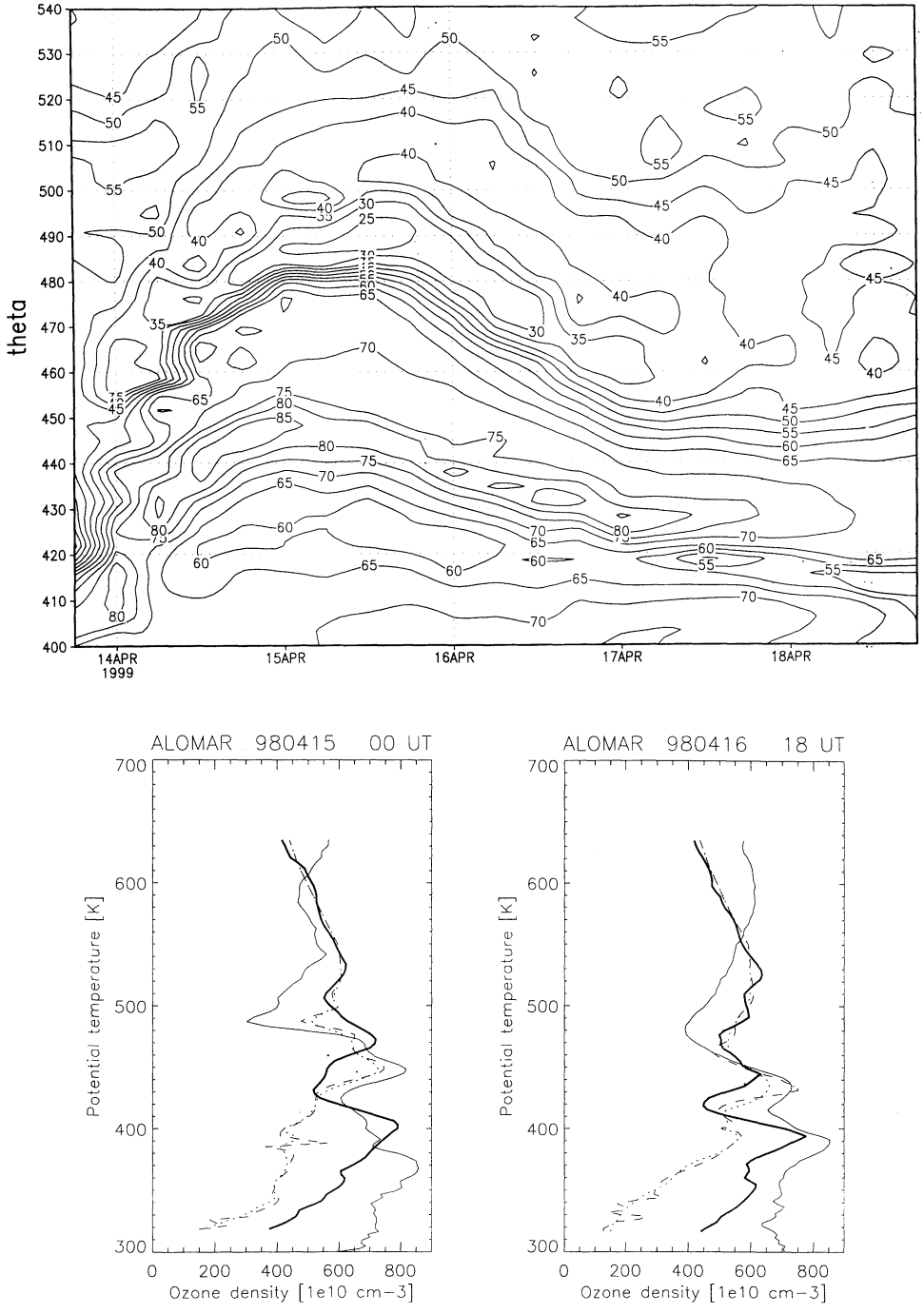

Figure 5. (top) Time evolution of the equivalent latitude (in degrees) reconstructed profile over April 13-18, showing multiple, ascending, and then descending laminae, near 440 K and 490 K. (bottom) Lidar and reconstructed ozone profiles on April 15-16, 1998 in the same format as Figure 1.

(Plate 1). The January 10 intrusion was also studied by Morgenstern and Carver [1999].

After mid-March, as the vortex breaks down, the ozone profiles are highly laminated. Numerous multiple laminae can be seen ascending or descending over a few days. Laminae that rapidly ascend or descend were first noticed in lidar observations by Orsolini et al. [1997]. Such multiple laminae are caused by "sandwiched" layers originating from different latitudes moving above Andoya. This is clearly seen in Figure 5 (top) which shows the time evolution of the equivalent latitude reconstructed profile over April 13-18. On April 15 and near 490 K, parcels originate from midlatitudes or subtropical latitudes, while in the bottom layer they originate at high equivalent latitudes, i.e., in the vortex, and have high ozone (see also Plate 1). Such mul-

tiple laminae were also observed by the lidar near April 15-16, 1998 (Figure 5) (bottom). There is a vertical offset between the modeled and observed structures, as model studies often reveal [Manney et al., 1998], but the observed maximum/minimum pair at 470 K/510 K on April 15 (OOOO UT) has clearly descended by April 16 (1800 UT).

5. Reconstruction of Column Ozone

In addition to reconstructing the ozone profile, we have calculated the 6-hourly model column ozone, using the analyzed pressure on the isentropes. A tropospheric contribution to total ozone of 30 Dobson Units (DU) is added. The contribution to column ozone from layers above 635 K is computed from the MLS daily mean observations, which extend to the stratopause. This contribution may amount from 20 to 50 DU.

Referring back to Figure 1, it can be seen that the model (thin line) reproduces the total ozone evolution throughout the winter and spring of 1997/1998: i.e., low values in early winter, high values in spring, and most remarkably, many fluctuations on day-to-day or week-to-week scales. Note the ozone drop in March.

Sharp total ozone peaks lasting 1-3 days are seen in the model (Figure 1), some largely in excess of 100 DU, especially in February and March. Lidar-derived total ozone values show at times sharp peaks (i.e. near day 55); the Brewer spectrometer also shows peaks of similar magnitude. The two most prominent ones in the model occurred on Julian days 46 and 61, i.e., February 15 and March 2 (see Figure 1). Very high total ozone, close to 500 DU, on Julian day 46 coincides with a pronounced lowering of low-level isentrope. This is clearly shown in Figure 6, where the pressure (in mbar) on the 300 K isentrope and total ozone are shown for January-February-March 1998. The mean equivalent latitude in the layer 300-420 K is also shown. In the midlatitudes, total ozone variability on synoptic time-scales is strongly related to storm track activity [Orsolini et al., 1998a] The ozone peaks found in the Andoya time series fits in the classical picture of depressed (elevated) tropopause being associated with high (low) total ozone: many of the model ozone peaks (Figure 6) coincide nicely with a lowered isentrope at 300 K. The amplitude of these peaks is modulated throughout spring/winter: they grow in amplitude from early December, reach maximum amplitude in February-March, and then decay (Figures 1 or 6). The lowered isentropes and associated high potential vorticity anomaly further coincide with high ozone mixing ratios in the lowermost levels. It is indeed in February that the ozone buildup

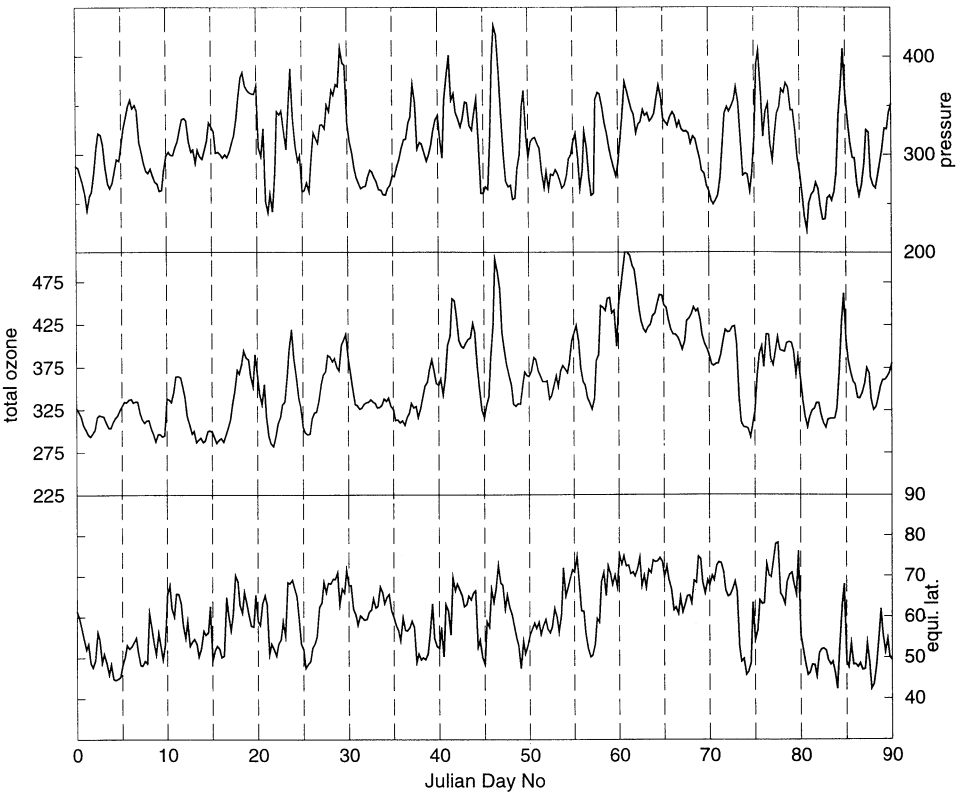

Figure 6. (top) Pressure (mbar) on the 300 K isentrope, (middle) model total ozone and (bottom) mean equivalent latitude in the layer 300-420K for January-February-March 1998. High ozone peaks coincide with lowering of the 300 K isentrope and high equivalent latitude above Andoya.

maximized at the bottom of the vortex: ozone mixing ratios between 425 K and 375 K from MLS were maximum in the first half of February, with the caveat that there were no MLS observations in March (Table 1). A notable exception to this simple paradigm occurs near March 2 (near Julian day 61), when the highest modeled column ozone was found. The 300 K isentrope was not extremely low; examination of Plate 1 shows that high ozone was then found in the entire lower stratosphere over a thick layer. This ozone peak was hence characterized by advection of ozone-rich air from high equivalent latitude over a deep layer, and the mean ozone content of the 300-375 K layer was the highest of the simulated period. The fact that there are few lidar observations during the model ozone peaks is consistent with the fact that they are associated with low tropopause and hence surface lows and enhanced cloud cover. On the opposite, low column ozone seen on several occasions between Julian days 70 and 90 can also be seen to be associated with periods of elevated 300 K isentrope and advection of air masses characterized by low equivalent latitude (Figure 6) and low ozone (see Plate 1 below 420 K, partial pressure between 6 and 15 mPa in blue shading).

6. Lamination Statistics

The frequency of occurrence and the mean amplitude of ozone laminae were examined in both lidar and reconstructed profiles. Laminae are hereinafter defined in a manner similar to that of Pierce and Grant [1998], i.e., fluctuations in the ozone mixing ratio exceeding 5% of the local mean ozone mixing ratio, with a vertical scale less than 2.5 km. A perturbation profile is obtained by substracting a mean vertical profile from the model or lidar profile.

The ozone is retrieved from the lidar every 300 m in the lower stratosphere, but its effective vertical resolution is 1.5 km. The laminae frequencies and amplitude were computed as a function of height and later converted to a mean potential temperature scale. The lidar profiles represent averages over several hours, typically 2 to 6, of observations. On the other hand, model profiles are expressed as a function of potential temperature and have an approximate resolution of 140 m (100 theta levels between approximately 9 km and 23 km). The model profiles were smoothed down to the lidar effective resolution. In Figure 7, a model profile for April 16, 1998 (1800 UT) is shown (thick solid line), along with the mean vertical profile (dashed-dotted line), the perturbation profiles (thin solid line) and the threshold values (dashed line). The circles at values of 1 or 0 indicate at which heights the laminae were counted or not on that specific day: i.e., the major multiple lamina was counted near 400 K-475 K and several smaller ones below 400 K. The counting algorithm searches for laminae, rich or poor in ozone. Sharp "cliffs" in the ozone profile can be counted as a pair of laminae.

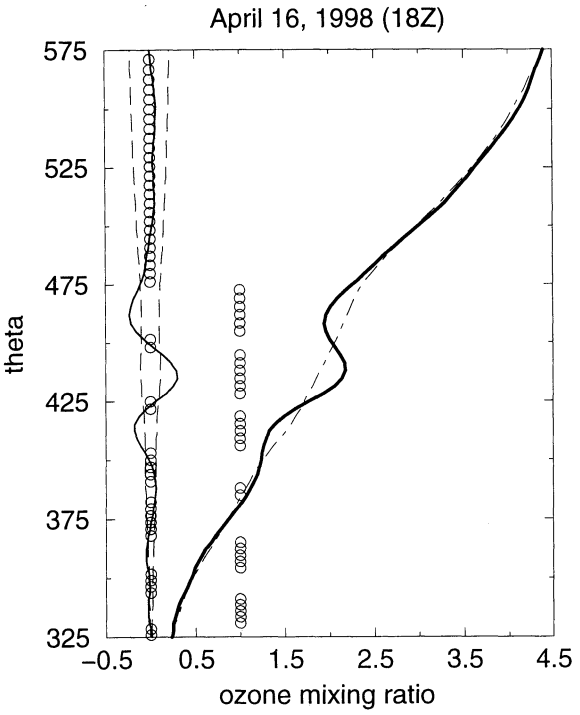

Figure 7. Model ozone profile (mixing ratio in ppmv) for April 16, 1998 (1800 UT) (thick solid line), along with the mean vertical profile (dashed-dotted line), the perturbation profiles (thin sodid line), and the threshold values (dashed lines). The circles at values of 1 or 0 indicate at which levels the laminae were counted or not.

Normalized frequency (f) of occurrence and mean amplitude are plotted as a function of potential temperature in Figure 8. A value of f equal to 0.4 indicates that 40% of the soundings display a lamina at that height. The mean amplitude is scaled by the mean ozone mixing ratio at that height.

Pierce and Grant [1998] analyzed a record of ozone sondes from a midlatitude site (Wallops Islands) and found that laminae were induced by both large-scale motions and by gravity waves. They were most abundant near 14-16 km (375 K-400 K). Averaged over winter and spring, laminae in excess of 10% of the local mean ozone had maximum frequency of occurrence of about 60% and a mean amplitude at about 10-15%. Bird et al. [1997] also estimated maximum lamination near 14-16 km in ozonesondes launched in the Canadian Arctic (80° N). From Figure 8, it appears that the lidar observations are consistent with maximum lamination in the layer 375 K-400 K. The mean occurrence and amplitude in the lidar profiles are less than those calculated by Pierce and Grant [1998], but more vertical structures are normally resolved by ozonesondes (vertical resolution of 50 m) than by the lidar. They estimated from the ozonesondes that laminae frequencies decreased below the 14-16 km maximum, especially in early winter. Our lidar measurements do not allow us to reliably examine laminations below 375 K. The model estimates

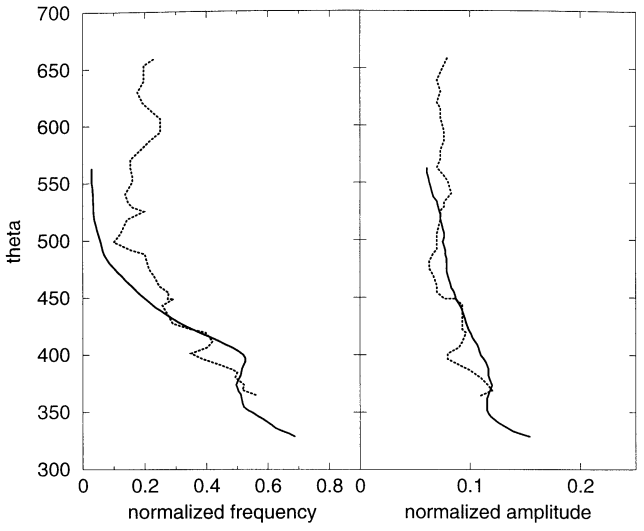

Figure 8. Laminae statistics for the winter and spring of 1997/1998: frequency of occurrence, normalized to 1, and laminae mean amplitude, scaled by the mean ozone mixing ratio, as a function of potential temperature, shown for the lidar observations (dotted lines), and the model (solid lines).

of laminae abundance and amplitude (Figure 8, solid line) only account for laminae induced by large-scale motions, as transport is isentropic and relies on analyzed winds. They are in rough agreement with the lidar estimates, but there seems to be enhanced lamination in the model near 400 K. The model laminae increase in amplitude and frequency below the 375-400 K layer, unlike the findings based on ozonesondes from Pierce and Grant [1998], Bird et al. [1997], or Reid and Vaughan [1991].

7. Discussion and Conclusions

Stratospheric ozone variability over the Arctic is large in winter and spring, from day-to-day to month-to-month scales. Ozone observations are, however, difficult to make especially in the Arctic winter. Ozone lidar observations are impaired by cloud cover and bad weather. Satellite determination of column ozone from reflected solar radiation is not possible in the polar night. The urgency to estimate the magnitude of Arctic ozone depletion has nevertheless increased the extent of the ground-based monitoring of stratospheric ozone in recent years.

Using meteorological analyses and global, but coarse and infrequent, MLS satellite observations, we have developed a modeling approach to reconstruct locally at Andoya, daily-varying ozone profiles and column. By "filling in" the temporal continuity of the ground-based observations, Lagrangian techniques help better understanding of the observed ozone variability.

To demonstrate the usefulness of this approach, a comparison has been made between reconstructed and observed ozone profiles, both time-mean and fluctuations, as well as total column.

As to total ozone, the continuous reconstructed time series over the winter and spring of 1997/1998 intercepts remarkably many of the scattered lidar estimations. Ozone peaks are seen in the model, lasting 1 to 3 days, in association with lowered isentropes near the tropopause and advection of ozone-rich air from the base of the vortex. A pattern of intensifying ozone peaks as the season progresses, culminating in February and March, is seen in both observation and model, although the model peaks seem to be more intense.

Laminae, i.e. thin layers typically less than 2-3 km, are produced in the model. The formation of ascending or descending laminae by large-scale advection is also captured. Their statistics in the model are in reasonable agreement with the lidar observations, except below 350 K, where the model produces more laminae. This might be due to the need of calculating three-dimensional diabatic trajectories near the tropopause.

However, filaments or laminae can be offset in altitude or time, with respect to observations, as commonly observed in such model studies [Fairlie et al., 1997; Manney et al., 1998]. It is difficult for the model to exactly position these small vertical structures. Potential sources for these discrepancies are the cumulative effect of errors in the wind fields, dependency on the length of the back trajectory and initialization techniques. The reconstructed ozone and, in particular, the column might show strong sensitivity to the initialization, which relies here on few observation points in both time and height.

Lagrangian methods such as the one presented in this paper are more and more used for interpretation and validation of satellite and ground-based observations. Further improvements to the method will be sought in the future. Improvement in the initial ozone data could be brought by combining data from different sources, such as various satellite instruments, ozonesondes, or aircraft observations. It is in the lowermost stratosphere that the initialization needs to be improved, as the MLS observations do not extend below about 14 km and hence had to be extrapolated downward.

Acknowledgments. This research was partially supported by the EU Commission Climate and Environment Programme (projects Meridional Transport of Ozone, and ENV4-CT95-0162), and by the Norwegian Research Council (project COZUV). Work at the Jet Propulsion Laboratory/California Institute of Technology was carried out under contract with the National Aeronautics and Space Administration. Supercomputing support to NILU was provided by a grant from the Norwegian Supercomputing Programme, and to JPL by the JPL/CalTech supercomputing project, funded by the NASA Offices of Earth Science, Aeronautics, and Space Science. We gratefully acknowledge Werner Eriksen and Reidar Lyngra for performing many of the lidar observations and the Andoya Rocket Range for their support.

References

Allen, D. R., and R. A. Reck, Daily variations in TOMS total ozone data, *J. Geophys. Res.*, *102*, 13,603-13,608, 1997.

Bird, J. C., S. R. Pal, A. I. Carswell, D. P. Donovan, G. L. Manney, J. M. Harris, and O. Uchino, Observations of ozone structures in the polar vortex, *J. Geophys. Res.*, *102*, 10,785-10,800, 1997.

Fairlie, T. D. A., R. B. Pierce, W. L. Grose, G. Lingenfelser, M. Loewenstein, and J. R. Podolske, Lagrangian forecasting during ASHOE/MAESA, *J. Geophys. Res.*, *102*, 13,169-13,182, 1997.

Froidevaux, L., et al., Global ozone observations from the UARS MLS: An overview of zonal-mean results, *J. Atmos. Sci.*, *51*, 2846-2866, 1994.

Froidevaux, L., et al., Validation of UARS Microwave Limb Sounder ozone measurements, *J. Geophys. Res.*, *101*, 10,017-10,060, 1996.

Hansen, G., and M. Chipperfield, Ozone depletion at the edge of the Arctic polar vortex 1996/1997, *J. Geophys. Res.*, *104*, 1837-1845, 1999.

Hansen, G., T. Svenoe, M. Chipperfield, A. Dahlback, and U.-P. Hoppe, Evidence of substantial ozone depletion in winter 1995/96 over northern Norway, *Geophys. Res. Lett.*, *24*, 799-802, 1997.

Hoppe, U.-P., G. Hansen, and D. Opsvik, Differential absorption lidar measurements of stratospheric ozone at ALOMAR: First results, *Eur. Space Agency Spec. Publ. SP370*, 335-344, 1995.

Manney, G. L., J. C. Bird, D. P. Donovan, T. J. Duck, J. A. Whiteway, S. R. Pal, and A. I. Carswell, Modeling ozone laminae in ground-based Arctic wintertime observations using trajectory calculations and satellite data, *J. Geophys. Res.*, *103*, 5797-5814, 1998.

Manney, G. L., H. A. Michelsen, M. L. Santee, M. R. Gunson, F. W. Irion, A. E. Roche, and N. J. Livesey, Polar vortex dynamics during spring and fall diagnosed using trace gas observations from the Atmospheric Trace Molecule Spectroscopy instrument, *J. Geophys. Res.*, *104*, 18,841-18,866, 1999.

Morgenstern, O., and G. D. Carver, Quantification of filaments penetrating the subtropical barrier , *J. Geophys. Res.*, *104*, 31,275-31,286, 1999.

Neuber, R., Nine years of polar ozone and aerosol observations at the German Arctic Station (Spitsbergen), edited by H. Wold et al., Proceedings of the 24th Annual European Meeting on Atmospheric Studies by Optical Methods, Andesnes, Norway, 1997.

Orsolini, Y. J., G. Hansen, U.-P. Hoppe, G. L. Manney, and K. H. Fricke, Dynamical modelling of wintertime lidar observations in the Arctic : Ozone laminae and ozone depletion. *Q. J. R. Meteorol. Soc.*, *123*, 785-800, 1997.

Orsolini, Y. J., D. B. Stephenson, and F. J. Doblas-Reyes, Storm track signature in total ozone in northern hemisphere winter, *Geophys. Res. Lett.*, *25*, 2413-2416, 1998a.

Orsolini, Y. J., G. L. Manney, A. Engel, J. Ovarlez, C. Claud, and L. Coy, Layering in stratospheric profiles of long-lived trace species: Balloon-borne observations and modeling, *J. Geophys. Res.*, *103*, 5815-5825, 1998b.

Pierce, R. B., and W. B. Grant, Seasonal evolution of Rossby and gravity wave induced laminae in ozonesonde data obtained from Wallops Island, Virginia, *Geophys. Res. Lett.*, *25*, 1859-1862, 1998.

Reid, S. J., and G. Vaughan, Lamination in ozone profiles in the lower stratosphere, *Q. J. R. Meteorol. Soc.*, *117*, 825-844, 1991.

Sutton, R. T., H. MacLean, R. Swinbank, A. O'Neill, and F. W. Taylor, High-resolution stratospheric tracer fields estimated from satellite observations using Lagrangian trajectory calculations, *J. Atmos. Sci.*, *51*, 2995-3005, 1994.

G. Hansen and Y.J. Orsolini, Norwegian Institute for Air Research (NILU), P.O. Box 100, N-2027 Kjeller, Norway. (ghh@nilu.no; orsolini@nilu.no)

N. Livesey and G.L. Manney, Jet Propulsion Laboratory, California Institute of Technology, 4800 Oak Grove Drive, Pasadena, CA 91109-8099, USA. (livesey@mls.jpl.nasa.gov; manney@iguana.jpl.nasa.gov)

U.-P. Hoppe, Norwegian Defence Research Establishment (FFI), P.O. Box 25, N-2027, Kjeller, Norway. (Ulf-Peter.Hoppe@ffi.no)

(Received February 17, 2000; revised September 28, 2000; accepted October 13, 2000.)